KUNS1463

Periodic-Orbit Bifurcation and Shell Structure at Exotic Deformation*

Ken-ichiro Arita, Ayumu Sugita* and Kenichi Matsuyanagi*
Department of Physics, Nagoya Institute of Technology, Nagoya 466, Japan
**Department of Physics, Graduate School of Science, Kyoto University, Kyoto 606-01, Japan*

Abstract

By means of periodic orbit theory and deformed cavity model, we have investigated semiclassical origin of superdeformed shell structure and also of reflection-asymmetric deformed shapes. Systematic analysis of quantum-classical correspondence reveals that bifurcation of equatorial orbits into three-dimensional ones play predominant role in the formation of these shell structures.

PACS number: 21.60.-n

1 Introduction

Shell structure, i.e., regular oscillating pattern in the smoothed single-particle level density, coarse-grained with respect to energy resolution, plays decisive role in determining shapes of finite Fermion systems [1–6]. According to the periodic-orbit theory [7–11] based on the semiclassical approximation to the path integral, shell structure is determined by classical periodic orbits with short periods. Finite Fermion systems like nuclei and metallic clusters favor such shapes at which prominent shell structures are formed and their Fermi surfaces lie in the valley of the oscillating level density, increasing their binding energies in this manner.

In this talk, we investigate the axially-symmetric deformed cavity model as a simple model of single-particle motions in nuclei and metallic clusters [8, 10, 12], and try to find the correspondence between quantum shell structure and classical periodic orbits. Our major purpose is to identify most important periodic orbits that determine major patterns of oscillating level densities at exotic deformations including prolate superdeformations, prolate hyperdeformations, oblate superdeformations and reflection-asymmetric shapes.

In the cavity model, the action integral S_γ for a periodic orbit γ is proportional to the length L_γ of it, $S_\gamma = \oint_\gamma \boldsymbol{p} \cdot d\boldsymbol{q} = \hbar k L_\gamma$, and the trace formula for the oscillating part of the level density is written as

$$\tilde{\rho}(E) \simeq \sum_\gamma A_\gamma k^{(d_\gamma - 2)/2} \cos(kL_\gamma - \pi\mu_\gamma/2), \tag{1}$$

where d_γ and μ_γ denote the degeneracy and the Maslov phase of the periodic orbit γ, respectively. Fourier transform $\tilde{F}(L)$ of $\tilde{\rho}(E)$ with respect to wave number k is

*Talk presented by K.M. at the International Symposium on *"Atomic Nuclei and Metallic Clusters: Finite Many-Fermion Systems"*, Prague, Sep. 1–5, 1997.

$$\tilde{F}(L) = \int dk\, k^{-(d-2)/2} e^{-ikL} \tilde{\rho}(E = \hbar^2 k^2/2M)$$
$$\simeq \sum_\gamma A'_\gamma \delta(L - L_\gamma), \tag{2}$$

which may be regarded as 'length spectrum' exhibiting peaks at lengths of individual periodic orbits. In the following, we shall make full use of the Fourier transforms in order to identify important periodic orbits.

We solve the Schrödinger equation for single-particle motions in the cavity under the Dirichlet boundary condition. We have constructed a computer program by which we can efficiently obtain a large number of eigenvalues as function of deformation parameters of the cavity [13]. We have systematically searched for classical periodic orbits in the three-dimensional(3D) cavities on the basis of the monodromy method [14].

2 Periodic-orbit bifurcations

As is well known, only linear and planar orbits exist in the spherical limit. When quadrupole deformation sets in, linear (diameter) orbits bifurcate into those along the major axis and along the minor axis. Likewise, planar orbits bifurcate into those in the meridian plane (containing the symmetry axis) and in the equatorial plane (perpendicular to the symmetry axis).

With variation of deformation, 3D and new 2D periodic orbits are successively born through bifurcations. Bifurcations that are important in the following discussions are
(i) bifurcations from multiple repetitions along the minor axis, which generate butterfly-shaped planar orbits in the meridian plane, and
(ii) bifurcations from multiple traversals of planar orbits in the equatorial plane, which generate 3D periodic orbits.

For prolate shapes (i) may be regarded as a limit of (ii), while this distinction is important for oblate shapes. We shall see that bifurcations of type (ii) are especially important for shell structure at prolate super- and hyper-deformations and at reflection-asymmetric shapes. Bifurcation points for (ii) are determined by stability of equatorial-plane orbits against small displacements in the longitudinal direction. Bifurcations occur when the following condition is met:

$$\frac{R_2}{R_1} = \frac{\sin(\pi t/p)^2}{\sin(\pi q/p)^2}, \tag{3}$$

where R_1 and R_2 denote the main curvature radii for the longitudinal and equatorial directions, respectively, and (p,t,q) are positive integers.

At the bifurcation points, trace of the (2×2) reduced monodromy matrix $\boldsymbol{M}$ representing stabilities of equatorial-plane orbits becomes $\mathrm{Tr}\,\boldsymbol{M} = 2$, indicating that they are of neutral stability at these points. The above equation was first derived by Balian and Bloch [8]. We note that, for the special case of prolate spheroidal shapes, R_2/R_1 is simply related to the axis ratio a/b as $R_2/R_1 = (a/b)^2$, a and b being lengths of the major and the minor axes, respectively, and (p,t,q) represent the numbers of vibrations or rotations of the periodic orbits with respect to the three spheroidal coordinates. They correspond to $(n_\epsilon, n_\phi, n_\xi)$ and (n_v, n_ϕ, n_u) of Refs. [10, 15], respectively. Periodic-orbit bifurcations in spheroidal cavities have been thoroughly studied by Nishioka et al.[15, 16]

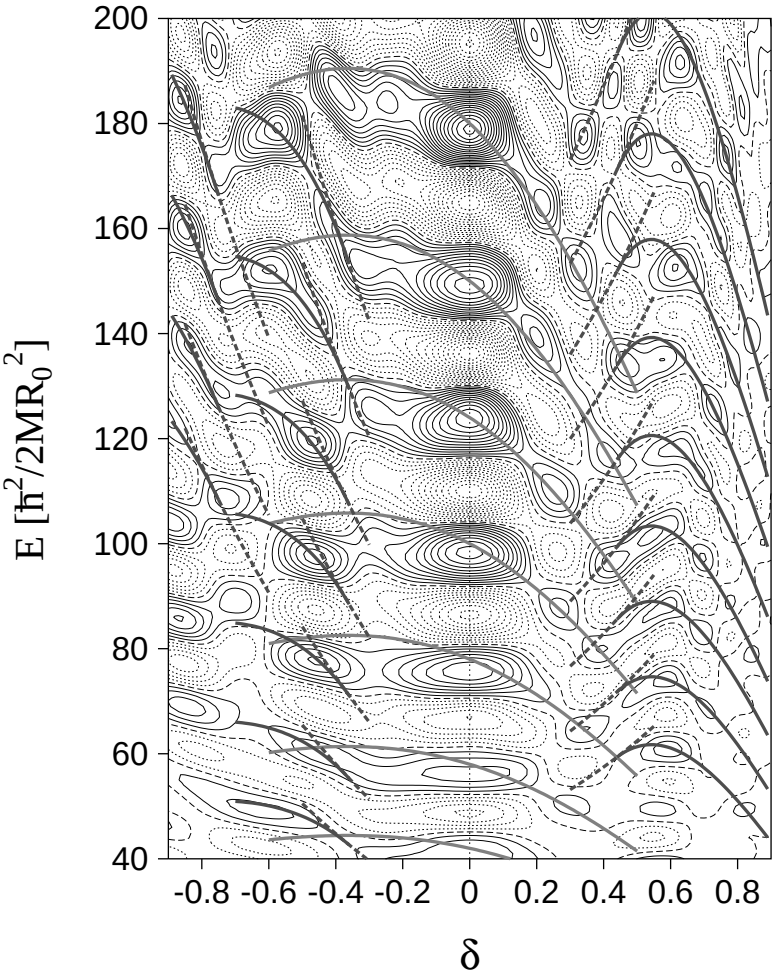

Figure 1: Oscillating parts of the smoothed level densities for spheroidal cavities, displayed as function of energy (in unit of $\hbar^2/2MR_0^2$) and deformation. Constant-action lines for some short periodic orbits are indicated by thick solid and broken lines (see text). The deformation parameter δ is related to the axis ratio $\eta \equiv a/b$ by $\delta = 3(\eta-1)/(2\eta+1)$ in the prolate case and by $\delta = -3(\eta-1)/(\eta+2)$ in the oblate case.

3 Semiclassical origin of superdeformations

Let us first discuss spheroidal cavities. In Fig. 1 oscillating parts of the smoothed level densities are displayed in a form of contour map with respect to energy and deformation. Regular patterns consisting of several valley-ridge structures are clearly seen. Thick solid and broken lines indicate constant-action lines for some important periodic orbits on which we are going to discuss. We here note that, as emphasized by Strutinsky et al.[10], if few families of orbits having almost the same values of action integral S_γ dominate in the sum in Eq. (1), the valleys in the contour map may follow such lines along which S_γ stay approximately constant.

Figure 2 displays Fourier transforms of the level densities. At normal deformation with $\delta = 0.3$, we notice peaks associated with triangular and quadrilateral orbits in the meridian plane.

Constant-action lines for the triangular orbits are indicated in Fig. 1 for several values of e_F that go through the spherical closed shells. It is clear that the valleys run along

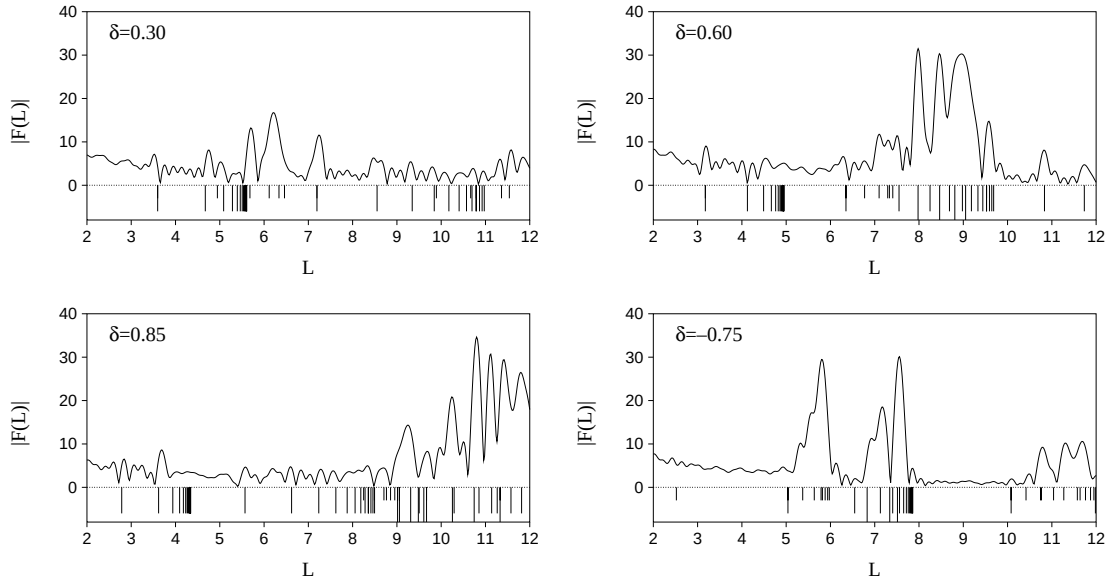

Figure 2: Fourier transforms of quantum level densities for spheroidal cavities with $\delta = 0.3$, 0.6 (prolate superdeformation), 0.85 (prolate hyperdeformation) and -0.75 (oblate superdeformation). In the bottoms of every figures, lengths (in unit of R_0) of classical periodic orbits are indicated by vertical lines. Long, middle and short vertical lines are used for 3D orbits, planar orbits in the equatorial and the meridian planes, respectively.

these lines.

With increasing deformation, bifurcations of linear and planar orbits in the equatorial plane successively take place [15]: Butterfly-shaped planar orbits with (p:t:q)=(4:2:1) bifurcate at $\delta \simeq 0.32$ from double repetitions of linear orbits along the minor axis. Then, 3D orbits (5:2:1) bifurcate at $\delta \simeq 0.44$ from five-point star-shaped orbits in the equatorial plane. Similar 3D orbits (6:2:1), (7:2:1), (8:2:1), etc. successively bifurcate from double traversals of triangular orbits, 7-point star-shaped orbits, double traversals of rectangular orbits, etc. in the equatorial plane. These 3D orbits form the prominent peaks seen in the range $L = 8 \sim 9$ in the Fourier transform for $\delta = 0.6$ (axis ratio 2:1).

Constant-action lines for the 3D orbits (5:2:1) are indicated by thick solid lines in the region $\delta \geq 0.44$ of Fig. 1. Good correspondence is found between these lines and shapes of the valleys seen in the superdeformed region. Constant-action lines for the other 3D orbits mentioned above also behave in the same fashion.

Some of these 3D orbits are displayed in Fig. 3. They possess similarities with figure-eight shaped orbits in the superdeformed harmonic oscillator with frequency ratio $\omega_\perp$:ω_z=2:1. An important difference between the the cavity model under consideration and the harmonic oscillator model should be noted, however: In the former they exist for all deformation parameters δ larger than the bifurcation points, whereas in the latter such periodic orbits appear only for special deformations corresponding to rational ratios of the major and the minor axes.[1]

On the other hand, Fourier peak heights associated with new orbits created by bifurcations quickly increase with increasing deformation and reach the maxima. Then, they start to decline. Thus, with variation of deformation, they are replaced by different peri-

[1] Note, however, that periodic orbits appear through bifurcations also for irrational ratios, if anharmonic terms like octupole deformations are added; see [17].

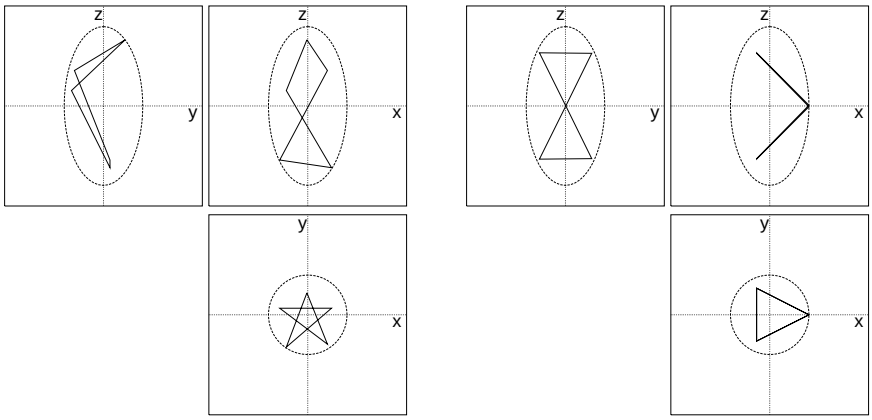

Figure 3: Three-dimensional orbits (5:2:1) and (6:2:1) in the superdeformed prolate cavity. Their projections on the (x, y), (y, z) and (z, x) planes are displayed.

odic orbits bifurcated later. We can confirm this, for instance, by comparing the Fourier transform for $\delta = 0.6$ (axis ratio 2:1) with that for $\delta = 0.85$ (axis ratio 3:1). In the latter, we see prominent peaks in the region $L = 11 \sim 12$ associated with 3D orbits (7:3:1), (8:3:1), (9:3:1) that are bifurcated, respectively, at $\delta \simeq 0.68, 0.73, 0, 76$ from 7-point, 8-point star-shaped orbits, and triple traversals of the triangular orbits in the equatorial plane. These 3D orbits resemble with Lissajous figures of the hyperdeformed harmonic oscillator with the frequency ratio 3:1.

For oblate spheroidal cavities with $\delta = -0.75$ (axis ratio 1:2), we see prominent peaks at $L \simeq 5.8$ associated with butterfly-shaped planar orbits (4:1:1), which are bifurcated at $\delta \simeq -0.36$ (axis ratio $1{:}\sqrt{2}$) from double repetitions of linear orbits along the minor axis. In addition, just at this shape, new planar orbits (6:1:1) bifurcate from triple repetitions of linear orbits along the minor axis [16]. We indeed see that a new peak associated with this bifurcation arises at $L \simeq 7.6$.

Constant-action lines for these bifurcated orbits (4:1:1) and (6:1:1) are indicated by thick solid lines in the region $\delta \leq -0.36$ of Fig. 1. We see clear correspondence between shapes of these lines and of valleys in the oscillating level density. Combining this good correspondence with the behavior of the Fourier peaks mentioned above, it is evident that these periodic orbits are responsible for the shell structure at oblate superdeformation.

The spheroidal cavities are special in that every bifurcated orbits form continuous families of degeneracy two, which means that we need two parameters to specify a single orbit among continuous set of orbits belonging to a family having a common value of action integral (length). We have checked [18], however, that the results obtained for spheroidal cavities persist also for other parameterizations of quadrupole shapes where the degeneracy is one. The present results for prolate normal- and super-deformations confirm the qualitative argument by Strutinsky et al.[10], except for the strong deformation dependence, found above, of relative contributions of different periodic orbits.

4 Reflection-asymmetric shapes

To explore the possibilities that significant shell structures emerge in the single-particle spectra for non-integrable Hamiltonians, we have carried out analysis of single-particle

Table 1: List of bifurcation points of important periodic orbits in the spheroidal cavity model. For more details, see Nishioka et al. [15, 16]

orbit (p:t:q)	axis ratio (a/b)	deformation δ	orbit length in R_0
(4:2:1)	1.41	0.32	7.1
(5:2:1)	1.62	0.44	8.1
(6:2:1)	1.73	0.49	8.7
(7:2:1)	1.80	0.52	9.0
(8:2:1)	1.85	0.54	9.2
(6:3:1)	2.0	0.6	9.5
(7:3:1)	2.26	0.68	10.3
(8:3:1)	2.42	0.73	10.9
(9:3:1)	2.53	0.76	11.4
(4:1:1)	1.41	-0.36	6.4
(6:1:1)	2.0	-0.73	7.6

motions in reflection-asymmetric cavities by parameterizing the surface as

$$R(\theta)/R_0 = \frac{1}{\sqrt{(\frac{\cos\theta}{a})^2 + (\frac{\sin\theta}{b})^2}} + a_3 Y_{30}(\theta), \tag{4}$$

When octupole deformation is added to the prolate shape (at normal deformation), spheroidal symmetry is broken and, accordingly, contribution of the triangular and quadrilateral orbits in the meridian plane decline. However, we have found that remarkable shell structure emerges for certain combinations of quadrupole and octupole deformations [17, 13]. As an example, Fig. 4 shows shell-structure energies calculated for $\delta = 0.1$ and $a_3 = 0.2$ with the Strutinsky procedure. Remarkable shell-energy gains are obtained by such deformations for systems above the spherical closed shells. This appears consistent with the result of realistic calculations by Frauendorf and Pashkevich [5] for shapes of sodium clusters.

Semiclassical origin of this quadrupole-octupole shell structure is again connected with bifurcation of 'equatorial'-plane orbits. Figure 5 shows the Fourier transform. We can clearly identify new peaks associated with orbits (3:1:1) and (4:1:1) bifurcated from trian-

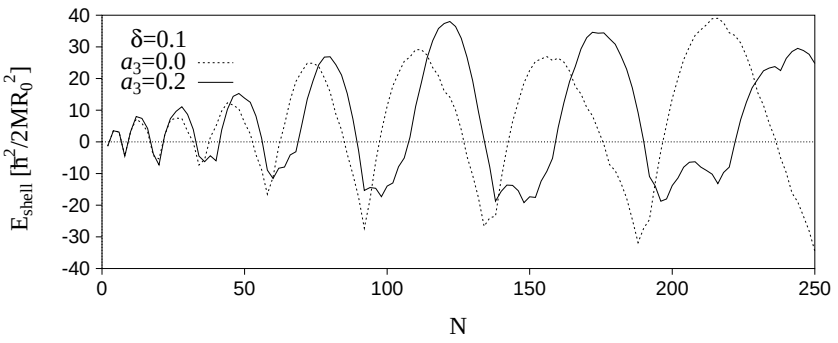

Figure 4: Shell structure energies (in unit of $\hbar^2/2MR_0^2$) of the reflection-asymmetric cavity with $\delta = 0.1$ and $a_3 = 0.2$, evaluated with the Strutinsky method and plotted as function of particle number N counting the spin degeneracy factor of two. For comparison, those for $\delta = 0.1$ and $a_3 = 0.0$ are plotted by broken lines.

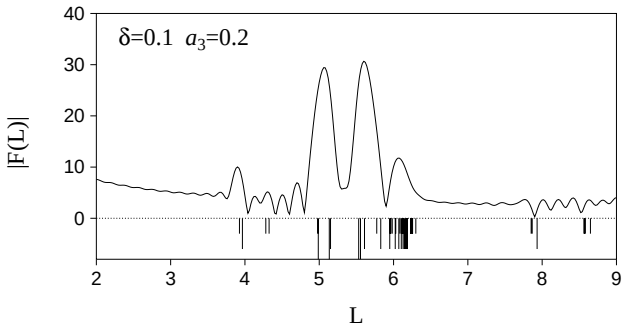

Figure 5: Same as Fig. 2, but for reflection-asymmetric cavity with $\delta = 0.1$ and $a_3 = 0.2$.

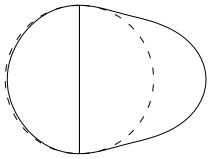

Figure 6: Illustration of a shape at the bifurcation point. A sphere tangent to the boundary at the 'equatorial' plane is indicated by a broken line.

gular and square orbits in the 'equatorial' plane at the center of the larger cluster of the pear-shaped cavity.

The key to understand the reason why bifurcations from 'equatorial'-plane orbits play important roles at finite octupole deformations may lie in the following point: Stability of these orbits is crucially dependent on the curvature of the boundary. The curvature radius in the longitudinal direction changes as the octupole deformation parameter a_3 varies, and at certain combinations of δ and a_3, it matches with the equatorial radius, as illustrated in Fig. 6. At this point, periodic orbits in the equatorial plane acquire *local spherical symmetry*, and form local continuous set of periodic orbits leaving from the 'equatorial' plane. This continuous set makes a coherent contribution to the trace integral and significantly enhances the amplitudes associated with these orbits. This is just the bifurcation point of orbits in the 'equatorial' plane, and 3D orbits bifurcate from the above local continuous set. One can readily check that for $R_2 = R_1$ all orbits ($p = 2, 3, 4, \ldots$) in the 'equatorial' plane simultaneously satisfy the bifurcation condition (3) with $t = q = 1$.

Some periodic orbits born out of these bifurcations are displayed in Fig. 7. Note that octupole deformations play crucial role in creating this kind of bifurcations, that occurs from a single turn ($t = 1$) of the 'equatorial'-plane orbits (it did not occur for quadrupole shapes).

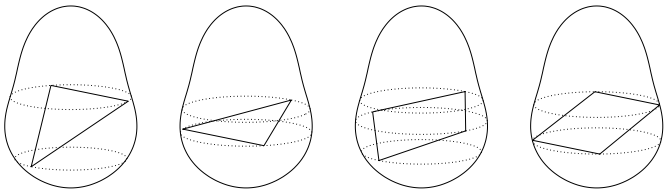

Figure 7: Some short periodic orbits bifurcated from 'equatorial'-plane orbits.

5 Conclusions

Classical periodic orbits responsible for the emergence of superdeformed shell structure for single-particle motions in spheroidal cavities are identified and their relative contributions to the shell structures are evaluated. Both prolate and oblate superdeformations as well as prolate hyperdeformations are investigated. Fourier transforms of quantum spectra clearly indicate that 3D periodic orbits born out of bifurcations of planar orbits in the equatorial plane become predominant at large prolate deformations, while butterfly-shaped planar orbits bifurcated from linear orbits along the minor axis are important at large oblate deformations.

We have also investigated shell structures for reflection-asymmetric cavities. It is found that remarkable shell structures emerge for certain combinations of quadrupole and octupole deformations. Fourier transforms of quantum spectra clearly indicate that bifurcations of triangular and square orbits in the 'equatorial' plane play crucial roles in the formation of these new shell structures.

References

[1] A. Bohr and B.R. Mottelson, *Nuclear Structure* (Benjamin, 1975) Vol. 2.

[2] S. Åberg, H. Flocard and W. Nazarewicz, Ann. Rev. Nucl. Part. Sci. 40 (1990) 439.

[3] P.A. Butler and W. Nazarewicz, Rev. Mod. Phys. 68 (1996) 349.

[4] I. Hamamoto, B. Mottelson, H. Xie and X.Z. Zhang, Z. Phys. D – Atoms, Molecules and Clusters 21 (1991) 163.

[5] S. Frauendorf and V.V. Pashkevich, Ann. Physik 5 (1996) 34

[6] W.D. Heiss, R.G. Nazmitdinov and S. Radu, Phys. Rev. B51(1995-I) 1874.

[7] M.C. Gutzwiller, J. Math. Phys. 12 (1971) 343.

[8] R. Balian and C. Bloch, Ann. Phys. 69 (1972) 76.

[9] M.V, Berry and M. Tabor, Proc. R. Soc. London A349 (1976) 101.

[10] V.M. Strutinsky, A.G. Magner, S.R. Ofengenden and T. Døssing, Z. Phys. A283 (1977) 269.

[11] M. Brack and R.K. Bhaduri, *Semiclassical Physics* (Addison-Wesley, Reading, 1997).

[12] H. Frisk, Nucl. Phys. A511 (1990) 309.

[13] A. Sugita, K. Arita and K. Matsuyanagi, preprint KUNS1431 (1997) and to be published.

[14] M. Baranger, K.T.R. Davies and J.H. Mahoney. Ann. Phys. 186 (1988) 95

[15] H. Nishioka, M. Ohta and S. Okai, Mem. Konan Univ., Sci. Ser., 38(2) (1991) 1.

[16] H. Nishioka, N. Nitanda, M. Ohta and S. Okai, Mem. Konan Univ., Sci. Ser., 39(2) (1992) 67.

[17] K. Arita and K. Matsuyanagi, Nucl. Phys. A592 (1995) 9.

[18] K. Arita A. Sugita and K. Matsuyanagi, to be published.